Design, Dynamic Simulation and Construction of a Hybrid HTS SMES for Chinese Power Grid

Jiahui Zhu[a,c], Ming Qiu[a], Bin Wei[a], Hongjie Zhang[a], Xiaokang Lai[a] and Weijia Yuan[b,*]

[a] *China Electric Power Research Institute, No.15 Xiaoying Road(East), Qinghe, Beijing 100192, China*
[b] *Department of Electronic and Electrical Engineering, University of Bath, United Kingdom*
[c] *Now as an academic visitor in the University of Bath, United Kingdom*

Abstract—High-temperature superconducting magnetic energy storage systems (HTS SMES) are an emerging technology with fast response and large power capacities which can address the challenges of growing power systems and ensure a reliable power supply. China Electric Power Research Institute (CEPRI) has developed a kJ-range, 20kW SMES using two state of art HTS conductors, BSCCO and YBCO tapes. This SMES system is used to compensate a power drop and a fluctuation in order to damp low frequency oscillations to increase stability of a power system. This paper presents an optimized design of the SMES system to achieve a maximum energy capacity. A voltage source converter using IGBTs is built and can be used to control the power flow between the SMES system and external circuits. A control system using a digital signal processor (DSP) and micro-programmed control unit (MCU) is constructed. SVPWM pulse modulation is used as a control strategy. The whole system was experimentally tested for compensation of power fluctuation within milliseconds in a dynamic power system simulation laboratory. The result validates the design and control circuit, and more importantly, the application capability of SMES systems in a power grid.

Key Words—BSCCO, dynamic simulation experiment, high temperature superconducting magnetic energy storage system(HT SMES), power fluctuation compensation, SWOT, YBCO.

I. INTRODUCTION

One emerging technology using superconductors is a SMES system which stores energy in the magnetic field produced by a persistent current in a superconducting loop. The advantages of SMES system compared with other energy storage system are, a) a significant larger power density than other energy storage system, b) a high cyclic efficiency (more than 85%), c) a substantially faster response speed than other technologies, d) infinite charge and discharge cycles [1-4]. Therefore, a SMES system would be ideal for power fluctuation compensation in a power grid to improve the power stability and quality. Since high temperature superconductors (HTS) have been developed significantly in the past decade, long lengths of two types of HTS conductors have been commercially available; Bi-2212 and Bi-2223 conductors (first generation HTS) and YBCO tapes (second generation HTS) [5] . Thus it is very attractive to use HTS conductors to build SMES systems to achieve larger energy/power densities.

There are several completed and ongoing HTS SMES projects for power system applications[6]. Chubu Electric has developed a 1MJ SMES system using Bi-2212 in 2004 for voltage stability[7]. Korean Electric Power Research Institute developed a 0.6MJ SMES system using Bi-2223 for voltage quality in 2007. In addition, they are now developing a 2.5MJ SMES system using YBCO conductors for power quality[8]. Superpower Inc, Houston University and Brookhaven National Lab began a 2G SMES project since 2011 and they are aiming to deliver a 2.5MJ system for load leveling in medium voltage 15-36 kV distribution networks.

China has a vast area and hence a unique power system structure. There are two crucial long-distance power transmission passages: West-to-East passage and North-to-South passage. The former passage delivers the electricity from the west to feed the majority of demand in the east. The latter passage includes the most important transmission line which enables the power flow exchange between the north and the south. This particular power grid structure usually leads to a number of problems including low frequency oscillation and power drop. CEPRI is the largest research institute in China in electrical power engineering, and also is the research-based subsidiary of State Grid Cooperation of China (SGCC). SGCC delivers 80% of China's electricity and has an annual research budget of £800 million pounds. Four years ago a £8million superconductivity research project including building a 1000m-long superconducting cable and a kJ-range HTS SMES system was awarded to CEPRI by SGCC since SGCC envisage superconductivity as a critical technology for future power grids[9].

This paper will give a comprehensive presentation of the SMES project supported by SGCC. We believe this is the first SMES system using 2G conductors to be constructed and tested in a power grid. The SMES using two different kinds of superconducting tapes, BSCCO and YBCO, is optimized to realize the maximum energy storage at 69K. Its cooling system is using sub-cooled LN2 to maintain cryogenic operation at 66K-77K. A quench protection unit which can detect partial active power is constructed. The LCL filtered voltage source power converter (VSC-based) system is designed and it has an AC/DC rectifier and a DC/DC chopper. A dual processor combined of DSP and MCU basing on a digital closed loop algorithm is used as a core controller. A real-time monitoring and display system acts as a host control center and interconnects each part of the SMES with data communication. Finally, a dynamic simulation and experiment using the hybrid HTS SMES for the power drop and fluctuation compensation is achieved. The results validate that the SMES can output the required compensation power and restrain the power fluctuation within milliseconds.

*Corresponding author. Tel.:+44 1225386049/7726759745;fax:+441225386305.
Email address: w.yuan@bath.ac.uk (Weijia Yuan).

II. VSC-BASED HYBRID HTS SMES CONFIGURATION

A. The Hybrid HTS Magnet Optimal Design

The critical currents of BSCCO and YBCO tapes in external magnetic fields have been tested. The measured I_c-B-θ curves of the BSCCO and the YBCO tapes at 77K are presented in Fig.1. As can be seen, the critical currents of BSCCO tapes decrease more than those of YBCO tapes in a same perpendicular magnetic field. Therefore we put the YBCO coils at the top and bottom ends of the SMES magnet because the perpendicular magnetic fields are higher in the top and bottom ends region. BSCCO coils are put in the middle of the SMES magnet where the perpendicular magnetic field is much smaller so that they can operate with high critical currents[10].

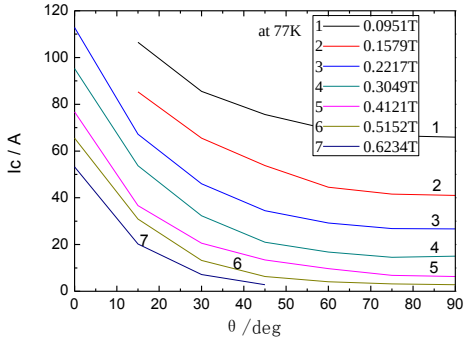

(a) BSCCO

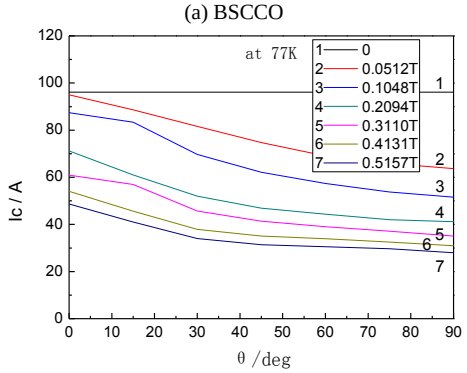

(b) YBCO

Fig. 1. Measured I_c-B-θ curves of HTS tapes.

Fig. 2. Photo of the hybrid SMES unit above the cryostat.

Fig. 2 presents the hybrid SMES unit which is going to be immersed in a sub-cooled LN2 cryostat. Based on the Stokes Theorem, the self and mutual inductances of each coil hence the stored energy can be calculated using Finite Element Method (FEM) [11-13]. An optimal design of the hybrid SMES magnet is achieved in order to maximize the operation current. Fig. 3 presents the flow chart of the optimization process. The maximum operation current I_{m1} of BSCCO coils and I_{m2} of YBCO coils are calculated by I_c-B-θ curves as shown in Fig.1. Since the BSCCO and YBCO coils are connected in series, the smaller one I_m between I_{m1} and I_{m2} is the possible maximum operation current for the whole magnet. k is the iteration number. In every iteration, $I_{m,k}$ is increased to $I_{m,k+1}$ using Eq.(2). The convergence criterion is presented by Eq. (3). The iteration will stop if OF is true.

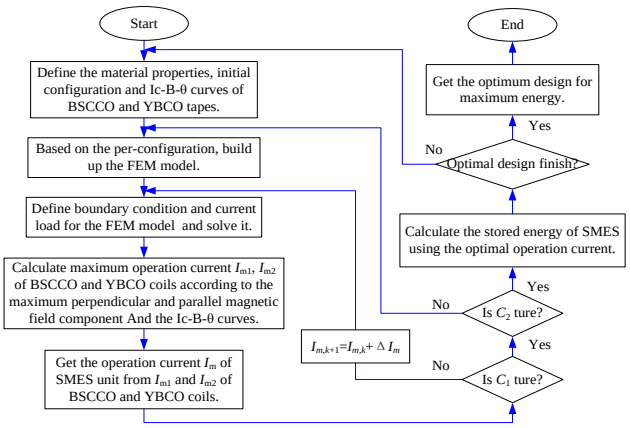

Fig. 3. Optimal design flowchart of hybrid SMES unit.

$$I_{m,k} = \min\left(I_{m1,k}, I_{m2,k}\right) \tag{1}$$

$$I_{m,k+1} = I_{m,k} + \varepsilon \cdot \left(I_{m,k+1} - I_{m,k}\right) \tag{2}$$

$$C_1 = \left|\frac{I_{m,k+1} - I_{m,k}}{I_{m,k}}\right| < 0.1, \quad C_2 = \left|\frac{I_{m,k+1}}{I_{c1}}\right| > 0.7 \cdot \tag{3}$$

$$OF = C_1 \wedge C_2 \tag{4}$$

The optimal configuration of the SMES coils is shown in Table 1. The operation current is 56 Amperes. The stored energy is 1.6 kJ at 77K and 6 kJ at 69K, respectively.

TABLE 1 OPTIMAL DESIGN OF THE HYBRID SMES

Specification	Quantity
Tape length (m)	2800
YBCO pancake number (12mm tape)	4
BSCCO pancake number (4mm tape)	20
Inner diameter (mm)	68
Outer diameter (mm)	222
Turns per YBCO pancake	450
Turns per BSCCO pancake	220
Total height (mm)	490
Inductance(H)	1.02
Operation current(A@77K/ A@69K)	56/109
Energy(kJ@77K/ kJ@69K)	1.6/6

B. Quench Detection and Protection

The quench protection for the hybrid HTS SMES is designed based the active power detection method which takes into account different positions of each YBCO and BSCCO pancake[14,15]. The voltage caused by the quench is detected and calculated by a voltage difference correction method, as shown in Fig.4.

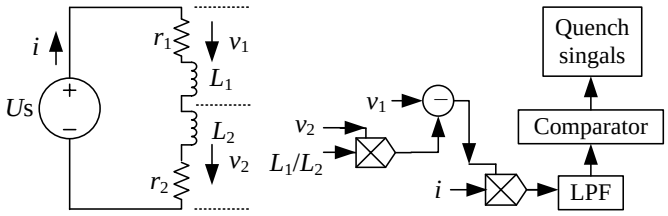

Fig. 4. Quench signal measurement diagram based on the voltage difference correction method.

L_1 are the inductance of an arbitrary double-pancake coil (the coil is X^{th} coil in the whole magnet from the top), L_2 are the inductance of the double-pancake coil which is the X^{th} coil in the whole magnet from the bottom. The active power P of the SMES can be calculated by Eq. (5), it can also be approximated by Eq.(6). The measurement circuit determines the quench condition by comparing the active power P_1 with quench threshold ΔU. Based on the actual operation condition of each superconducting coil,

the quench threshold ΔU can be calculated by Eq. (7). Because the quench resistance is usually very small, ΔU can be defined as 200mV.

$$P=[(L_1-L_2)di/dt+(r_1-r_2)i]i=[(L_1-L_2)di/dt]i+(r_1-r_2)i^2 \tag{5}$$

$$P_1=K[v_1-(L_1/L_2)v_2]i \tag{6}$$

$$\Delta U=Kr_1i^2-K[r_1-(L_1/L_2)r_2]i^2=K(L_1/L_2)r_2i^2 \tag{7}$$

In Eq. (5) and Eq. (6), r_1 and r_2 are the resistance of two coils after quench taking place; K is a constant which is determined by the electrical parameters of the measurement circuit; i is the operation current of SMES.

The quench signal measurement circuit is presented in Fig.5. The quench signal is sent to the quench protection hardware circuit to drive the power electronic switch and to provide the energy releasing circuit for SMES, as Fig.6.

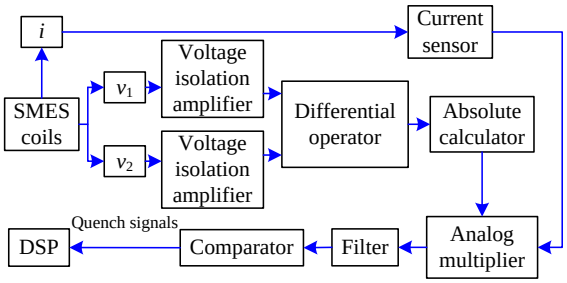

Fig. 5. Operation principle and components of quench measurement circuit.

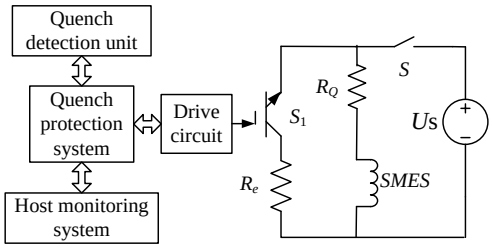

Fig. 6. Quench protection circuit for the hybrid SMES.

C. *The LCL Filtered VSC-SMES Power Conversion*

A double loop control strategy (both voltage and current) is used to control VSC-based converter[16-18]. Fig. 7 shows the power compensation process. If the power fluctuation is P_{Bus1} at Bus1, the compensation power P_{inj} can be calculated with reference values of the active current i_d^* and the reactive current i_q^*. i_q^* is defined as zero, thus achieving a unity power factor in the energy exchange process as shown in Eq.(8).

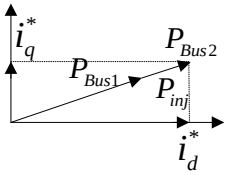

Fig. 7. Vector diagrams of the compensation power.

The outer loop of the control strategy controls the voltage on the DC side using the numerical PI (Proportional Integral) anti-saturation algorithm[19]. Then according to the compensation power, as reference values of i_d^* and i_q^*, required in power system, the compensation currents in d and q axis components of $\triangle i_d$ and $\triangle i_q$ are in Eq.(9).

$$\begin{cases} i_d^*=\left(K_{uP}+\dfrac{K_{uI}}{s}\right)\left(u_{dc}^*-u_{dc}\right) \\ i_q^*=0 \end{cases} \tag{8}$$

$$\begin{bmatrix}\Delta i_d\\ \Delta i_q\end{bmatrix}=\begin{bmatrix}i_d^*-i_d\\ i_q^*-i_q\end{bmatrix} \tag{9}$$

K_{uP} , K_{uI} are the PI control factors in DC voltage loop; s is Laplace operator; u_{dc} is the converter sampling value of DC voltage;

u^*_{dc} is the reference DC voltage value of converter; U_k, $i_k(k=a,b,c)$ are the d and q axis components (U_d, U_q, I_d, I_q) of three phase sampling voltages (U_a, U_b, U_c) and currents (I_a, I_b, I_c).

A synchronous PI control algorithm is used in the inner current loop control strategy to adjust current to achieve zero steady-state error and a sinusoidal distribution. The rated voltage values of v_d and v_q are as follows. The three phase compensation voltage $U_{kout}(k=a,b,c)$ are generated by (11) to drive the IGBTs in the converter.

$$\begin{cases} v_{\mathrm{d}} = -(K_p + \dfrac{K_i}{s})\Delta i_{\mathrm{d}} + u_{\mathrm{d}} \\ v_{\mathrm{q}} = -(K_p + \dfrac{K_i}{s})\Delta i_{\mathrm{q}} + u_{\mathrm{q}} \end{cases} \tag{10}$$

$$[U_{aout}, U_{bout}, U_{cout}]^{\mathrm{T}} = T_{dq/abc}[v_d, v_q]^{\mathrm{T}} \tag{11}$$

K_p, K_i are the PI control factors; $T_{dq/abc}$ is a coordinate transformation matrix.

In addition, a synchronous control method for charging and discharging the chopper is proposed. The small-signal function of SMES current i_{smes} in charging mode is shown in Eq.(12) and the small-signal function of DC voltage u_{dc} in discharging mode is shown in Eq.(13). Then the SVPWM pulses are generated according to the voltage u_{dc} and SMES current i_{smes} to drive the IGBTs in the chopper.

$$\hat{i}_{smes} = \frac{u_{dc}}{Ls + R_{sc}} \hat{d}_8 \tag{12}$$

$$\hat{u}_{\mathrm{dc}} = -\frac{R_L i_{sc}}{CR_L s + 1} \hat{d}_7 \tag{13}$$

$\hat{i}_{sc}$, $\hat{u}_{dc}$, $\hat{d}_7$, $\hat{d}_8$ are the disturbance quantities of SMES current, DC side voltage, cycle duty of the power component S_7 and S_8, seen in Fig.8.

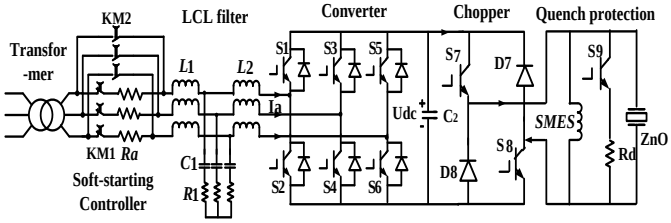

Fig.8. Topology diagram of the SMES converter circuit.

Fig. 8 shows the converter topology for the SMES. It includes a soft-starting controller, LCL filter, three-phase half-bridge voltage converter, chopper and quench protection circuit. By using this converter, the circuits can be operated in charging, discharging, persistent and quench protection modes by controlling the power electronic switches S1- S9.

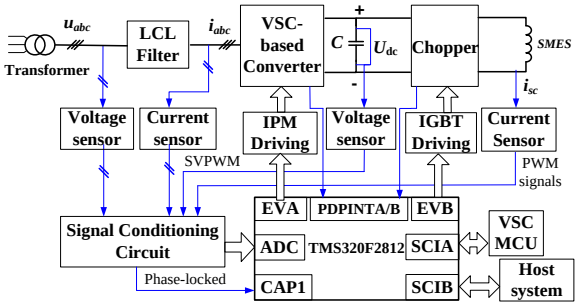

Fig.9. Converter control circuit based on DSP TMS320F2812.

Fig.9 presents the control circuit of the VSC-based power converter. It consists of a main power circuit, DSP control circuit, signals sampling, conditioning and driving circuit and monitoring terminals. A 32 fixed point, 150 MHz TMS320F2812 DSP chip acts as a central control unit and a micro-programmed control unit (MCU) C8051F020 acts as a visual monitoring and I/O unit for the converter.

This power converter can isolate the SMES magnet from the power system and improve the stability and efficiency of the SMES power conversion due to the chopper.

D. The host control and monitoring System

Based on the virtual instrument technology and multi-threaded modular design method, we have built up a host control and monitoring system for the hybrid SMES. The host system visualizes the performance of each component in the SMES system and

is easy to be expanded and adapted[20]. It can not only communicate with the superconducting magnet, sub-cooled LN2 cryogenic system, quench protection and power conversion units but can also monitor in real-time the power grid condition in order to operate the SMES system.

Fig.10 illustrates the configuration of the SMES host system. The information data is transferred to the host monitoring and controlling system by LAN and RS232. Its hardware circuit includes a measurement unit, a serial detection unit, a wave recording unit and a control unit. The measurement unit monitors the power grid conditions i.e. the three-phase voltages and currents. The serial detection unit monitors the SMES system. All the operation information can be recorded by the wave recording unit. Based on the operation conditions of the power grid and SMES, the control unit in the host system of SMES is able to operate the SMES unit in charge, persistent or discharge in order to compensate the power fluctuation.

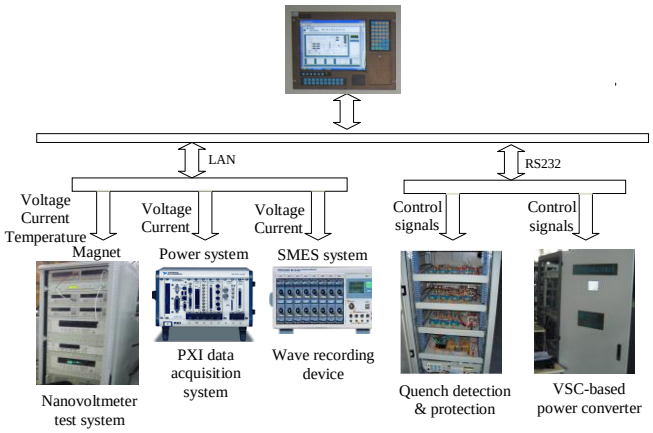

Fig.10. Host monitoring and controlling system diagram.

If a fault occurs in the SMES system, the fault signal will be transferred to the host monitoring and controlling system by RS232. The priority for responding to the fault signal can be determined by the host system. The quench protection signal is defined as the highest priority. When it is sent to the host monitoring and controlling system, the stop command is sent to the quench protection circuit, the power converter circuit and then the cooling system. All of SMES system will disconnect from the power grid. The priority is FO1>FO2>FO3; the response sequence of each module in the SMES is shown in Fig.11 (according to the priority order given by the host monitoring and controlling system).

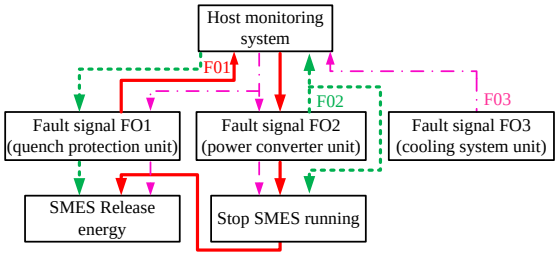

Fig.11. Response priority of each modular in the hybrid SEMS.

III. Dynamic Simulation of the VSC-based SMES

The active and reactive power conversion in four-quadrant between the SMES and the power system is simulated in Matlab / Simulink environment to validate the control strategy of the hybrid SMES system.

There are three operation modes for the SMES: charging, persistent and discharging. In charge mode, the chopper uses the current-cycle control strategy and the VSC operates as a rectifier to charge the SMES system[21,22]. When the current reaches the rated value, the SMES system will be switched into the persistent mode to keep its current at a constant value hence store the energy. Fig.12 gives a simulation result of the SMES system which is firstly in the charging mode and then switched into the persistent mode. The DC side voltage, 3-phase voltage and current simulation waveforms in the power system in real time can be seen in Fig.12.

In the discharging mode, the chopper uses a voltage-cycle control strategy and the VSC operates as an inverter to release the energy to the power system. Fig.13 gives the simulation result in discharging mode. In Fig.13, SMES transfer its energy to the power system at two different discharge speeds.

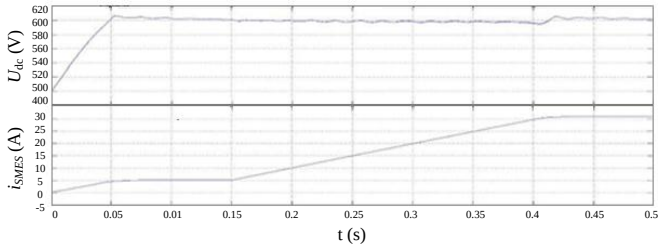

(a) Voltage and current simulation waveform of SMES in the charging mode (0-0.41s) and also persistent mode (from 0.41s)

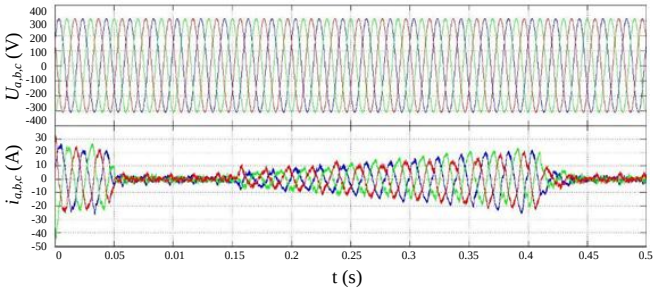

(b) 3-phase voltage and current simulation waveforms in the charging mode (0-0.41s) and also persistent mode (from 0.41s)

Fig.12 The charging and persistent mode simulation results.

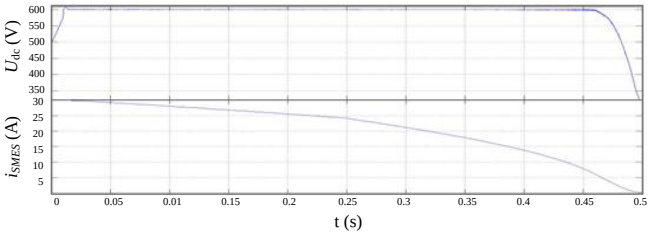

(a) Voltage and current simulation waveform of SMES in discharging mode

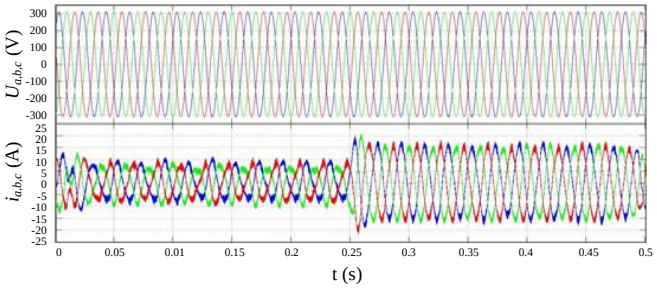

(b) 3-phase voltage and current simulation waveforms in discharging mode

Fig.13 The discharging model simulation results.

IV. Experiment Connected in a Power Grid

A. SMES Experimental System

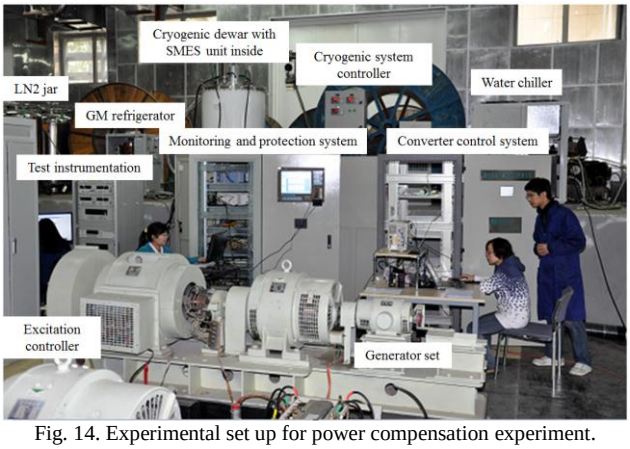

Fig. 14. Experimental set up for power compensation experiment.

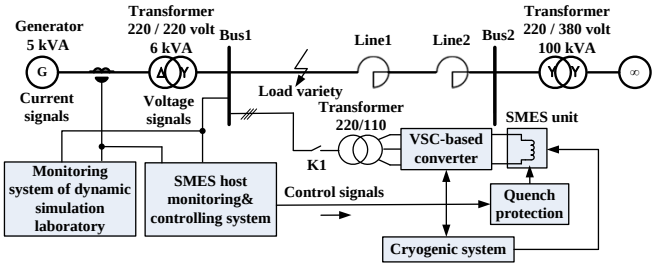

Fig. 15. Circuit diagram of the power compensation experiment.

A grid-connected test system for power compensation experiment using the hybrid SMES system is constructed in the dynamic simulation laboratory of State Grid Corporation of China, as seen in Fig.14. The transmission power system simulates a real power system and its parameters are designed according to the ratio of actual parameters, as shown in Fig.15. It consists of a 200 km line (Line1 and Line2), 5kVA generator, 6kVA transformer, 100kVA system transformer and a 3kW controllable load. The SMES system is connected to the system at Bus1. The SMES system consists of a monitoring and controlling system, a magnet unit, a cryogenic system, a power converter and a quench protection system. The SMES unit is placed in a dewar filled with LN2. The SMES unit is connected to a GM refrigerator with a cooling capacity of 600W at 77K, hence can be the further cooled down to 65K. The dynamic simulation laboratory has its own monitoring and controlling system for the power grid and thus can record the real-time operation data on power transmission lines.

B. Experimental Results and Analysis

1) Power drop compensation

For quantitative analysis of the SMES characteristics for power drop compensation, a 5kW power drop was imposed at Bus1 by removing all of the loads in the power transmission line for 300ms. The SMES system began to deliver energy 25ms after the power drop. The time delay is due to the communications between the host system and the converter. Fig. 16 presents the experimental waveforms of phase-A current, phase-A inverter current and the SMES system current during the power drop compensation. As can be seen in Fig. 16, the SMES unit current i_{SMES} decreases from 50A to zero. An inverter current i_{a_inv} is generated by the converter with a maximum instantaneous value at 20A. It took the SMES unit 625ms to fully release its energy, which is sent to the power grid to compensate the power drop. Therefore the 3-phase currents in power system have been compensated.

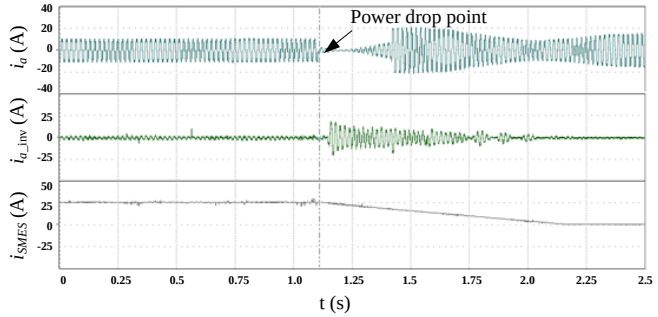

Fig. 16 The experimental waveforms of phase-A current, the phase-A inverter current and the SMES unit current in the power compensation experiment.

The electric power waveforms before and after compensation is shown in Fig.17. The maximum and minimum electric power in power drop period is compared in Table 2. Because the magnitude of power drop generated in the power transmission line is more than the energy capacity of the SMES system, the power drop cannot be fully compensated. If the energy capacity of the SMES system is large enough, the power drop would be fully compensated. In Table 2, the transmission power on the transmission line is 1.07kW at the end of the power drop period without compensation; however, it increases 1.4 times to 1.5kW with the SMES energy for compensation. It validates that the SMES system is able to compensate power drop and improve power quality.

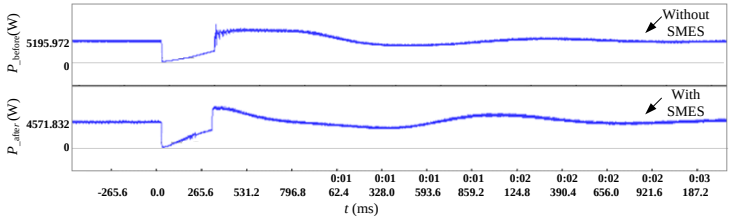

Fig. 17. Electric power in the power transmission line comparison before and after using the SMES system.

TABLE 2 COMPARISON OF THE TRANSMISSION POWER IN THE POWER DROP PERIOD WITH AND WITHOUT SMES

Electric power(kW)	Without SMES	With SMES
Minimum value Smin (kW)	0	0
Maximum value Smax (kW)	1.07	1.5

2) Power fluctuation compensation

A 3kW load was removed for 160ms on Bus1 at t=0.25s to generate a power fluctuation fault. The transient power is monitored at 5kHz sampling rate and is compared with the reference power. The host monitoring and control system drives the SMES to produce the power to compensate the oscillation.

In this experiment, the SMES system began to charge from 100ms after the load dump occurs. It was firstly in charging mode for 350ms, then in persistent mode for 30ms and discharging mode for 600ms. Thus the load power is maintained at the normal value on Bus1. Experimental waveforms of the inverter current of phase A and the current of the SMES unit are shown in Fig.18. The three-phase powers *P* with and without SMES on the power transmission line are shown in Fig.19.

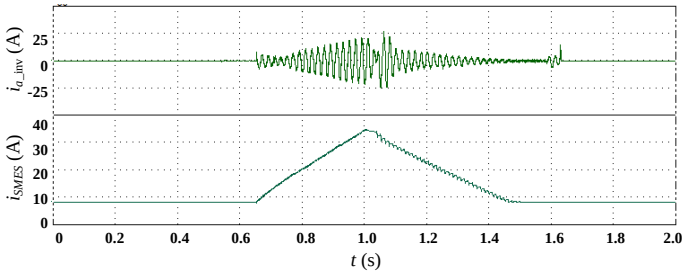

Fig. 18. Experiment waveforms of phase-A inverter current and SMES current.

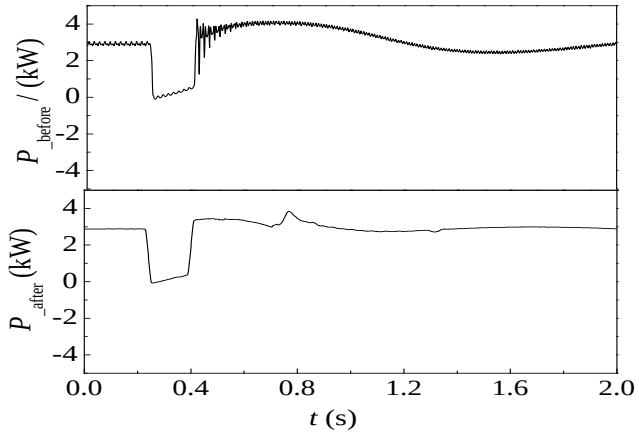

Fig. 19. Experiment waveforms of three-phase power *P* without and with SMES compensation.

The maximum power fluctuation ratio k_p is defined as follows,

$$k_p = \frac{\max(P - P_N)}{P_N} \cdot 100\% \tag{14}$$

Where *P* is the transient power value, P_N is the rated power.

As can be seen from Table 3, without compensation the power fluctuation peak-to-peak value is 1.72 kW and the power fluctuation ratio is 37.8%. After compensation, the power fluctuation peak-to-peak value is reduced to 0.53kW and the power fluctuation ratio is reduced to 14.5%, a 69.4% reduction compared with no SMES case. Although there are little spikes in the compensation process since the high-frequency harmonics cannot be completely filtered by the filter in the real experimental setup, the SMES system compensates the power oscillation fluctuation efficiently.

TABLE 3 COMPARISON OF ELECTRIC POWER FLUCTUATION BEFORE AND AFTER COMPENSATION

SMES operation mode	Rated Power P_N /kW	Power value *P* /kW			
		Minimum power P_{min}	Maximum power P_{max}	Peak-to-peak power	power fluctuation ratio k_p
Without SMES	3	2.4	4.13	1.73	37.8%
With SEMS	3	2.9	3. 43	0.53	14.5%

C. *Discussion of Application Prospect of SMES Systems to Power Grids in Future*

The dynamic simulation experiment is able to simulate a real power grid by scaling down the real system parameters accordingly. This dynamic experiment simulates a real power grid which includes, a) a 200 km-long, 110kV double-side power transmission line with 0.4 Ohm resistance per km; b) a 530MW generator; c) with an infinite short-circuit capacity 600MVA.In the dynamic simulation experiment, the maximum instantaneous output power of SMES is 3.5kW. It is equivalent to 371MW in the double-side

transmission line system according to the power conversion coefficient of the generator in the experimental system. Therefore, the SMES unit energy is equivalent to 100 MJ at 69K. It can be concluded that the capacity of a SMES unit needs to reach the range of hundreds of MJ for power drop compensation in an 110kV transmission power system. Scaling up the SMES capacity and increasing the power conversation speed are the most crucial factors in applications of SMES systems to power grids. For the future prospect application in power grids, the Strengths, Weaknesses, Opportunities and Threats (SWOT) analysis of HTS SMES systems is presented in Table 4.

TABLE 4 SWOT ANALYSES OF HTS SMES SYSTEMS FOR POWER APPLICATIONS

	Positive	**Negative**
Internal factors	Strengths • Response speed within millisecond • Larger power density • Efficiency above 95% • Infinite charge and discharge cycles • No mechanically moving parts, little maintenance required	Weaknesses • Expensive material and cooling cost • Self-discharge in several days due to no persistent switch • Low energy density • Instability of superconductors in the loss of cooling power
External factors	Opportunities • High operation temperature to reduce the cryogenic cost • Large current and energy density due to 2G HTS technologies • Small-scale system used for oscillation damping, flicker diminishing, power factor correction	Threats • Impact on the traditional electric device • Health risk caused by the stray magnetic field • Instability of cooling systems (evaporation of liquid cryogen, burst of vacuum space)

V. CONCLUSION

We have successfully built up a VSC-based hybrid HTS SMES unit which includes the hybrid magnet using YBCO and BSCCO tapes, cryogenic system with sub-cooled LN2, power converter with LCL filter, quench protection circuit and monitoring and controlling system. This is the first HTS SMES system to be operated in sub-cooled LN2 in a dynamic power system laboratory. A novel quench detection and position protection system has been developed. In addition, a visualized converter control system and online host monitoring and protection system have been constructed.

The power drop and fluctuation compensation algorithm is designed based on the dual of DSP and MCU. A power transmission system was set up in the dynamic power system simulation laboratory. This laboratory system is equivalent to a 200km long 110kV transmission line in a real power grid. The SMES system was successfully operated in two different experiments, power drop compensation and power oscillation compensation. The experimental results have validated the design and control strategy of the SMES unit. More importantly, it validates that the SMES system is able to improve the power quality with a fast response speed for a power grid. The future work includes scaling up the SMES system and increasing its response speed for large-scale applications.

ACKNOWLEDGMENT

Jiahui Zhu and Weijia Yuan would like to thank the support by Royal Academy of Engineering Research Exchanges with China Scheme, UK and the National Natural Science Foundation of China (Grant No. 51207146). All the Authors would like to acknowledge the dynamic simulation laboratory of the State Grid Corporation of China for their active support in the experiment.

REFERENCES

[1] M. H. Ali.. An overview of SMES applications in power and energy systems. IEEE Trans. Sustainable Energy 2010; 1: 38-47.
[2] Y.M. Kim, D.G. Shin, D. Favrat. Operating characteristics of constant-pressure compressed air energy storage (CAES) system combined with pumped hydro storage based on energy and exergy analysis. Energy 2011; 36(10):6220-6233.
[3] Matteo Morandin, François Maréchal, Mehmet Mercangöz, Florian Buchter. Conceptual design of a thermo-electrical energy storage system based on heat integration of thermodynamic cycles - Part B: Alternative system configurations. Energy 2012; 45(1):386-396.
[4] S. Padrón, J.F. Medina, A. Rodríguez. Analysis of a pumped storage system to increase the penetration level of renewable energy in isolated power systems. Gran Canaria: A case study. Energy 2011; 36(12):6753-6762.
[5] D. Larbalestier, A. Gurevich, D. M. Feldmann, A. Polyanskii. High Tc superconducting materials for electric power applications, Nature 2001; 414:368-377.
[6] Shinichi Nomura, Naruaki Watanabe, Chisato Suzuki, Hiroki Ajikawa, Michio Uyama, Shinya Kajita, et, al. Advanced configuration of superconducting magnetic energy storage. Energy 2005; 30(11-12): 2115-2127.
[7] Nagaya, S., Hirano, N., Shikimachi, K. Development of MJ-class HTS SMES for bridging instantaneous voltage dips. IEEE Transactions on Applied Superconductivity 2004;14(2):770 – 773.
[8] Myungjin Park, Sangyeop Kwak, Wooseok Kim. Conceptual design of HTS magnet for a 5 MJ Class SMES. IEEE Transactions on Applied Superconductivity 2008; 18(2): 750 - 753.
[9] Zhu jiahui, Qiu Ming, Wei Bin, Zhang Hongjie. Research on the second generation high temperature superconducting magnetic energy storage system. In Proc. 5th General Meeting / 7th Technical Meeting of Powe System between China, Japan and Korea. Chang Won, Korea; September 2009.
[10] Jiahui Zhu, Weijia Yuan, T.A. Coombs, Q. Ming. Simulation and experiment of a YBCO SMES prototype in a voltage sag compensation. Physic C 2011; 471(5-6):199-204.
[11] Cho, J.W. Fabrication and test of a 3MJ SMES magnet. IEEE Transactions on Applied Superconductivity 2004;14: 743 - 745.
[12] Noguchi, S., Ishiyama, A., Akita, S., Kasahara, H., Tatsuta, Y., Kouso, S. An optimal configuration design method for HTS-SMES coils. IEEE Transactions on Applied Superconductivity 2005; 15(2):1927 - 1930.
[13] JiahuiZhu, Qiang Cheng, Bin Yang, Weijia Yuan, T.A. Coombs, Ming Qiu. Experimental research on dynamic voltage sag compensation using 2G HTS SMES. IEEE Trans. on Applied Superconductivity 2011; 21(3): 2126 - 2130.
[14] Bin Wei, Yanfang Yang, Ming Qiu, Hongjie Zhang, Jiahui Zhu, Panpan Chen, Dongxu Zhu, Xiaokang Lai. The quench detection system for YBCO superconducting magnets. IEEE Trans. on Applied Superconductivity 2010; 20(3):1361-372.
[15] Ueda, H. , Aoki, Y. , Shikimachi, K. , Hirano, N. , Nagaya, S. Quench behavior and protection in cryocooler-cooled YBCO pancake coil for SMES. IEEE Transactions on Applied Superconductivity 2011; 21(3):2398 -2401.

[16] Jiahui Zhu, Xuzheng Bao, Bin Yang, Panpan Chen, Yanfang Yang, Ming Qiu. Dynamic simulation test research on power fluctuation compensation using hybrid SMES of YBCO and BSCCO tapes. IEEE Trans. on Applied Superconductivity 2012; 22(3): 5700404.
[17] Jing Shi, Yuejing Tang, Tao Yao, Jingdong Li, Shijie Chen. Study on control method of voltage source power conditioning system for SMES. In Proc. IEEE/PES Trans. Distribution Conf. & Exhibition, Asia and Pacific Dalian, China; 2005.
[18] Christof Humpert. Long distance transmission systems for the future electricity supply - Analysis of possibilities and restrictions. Energy, In Press, Corrected Proof, Available online 18 July 2012
[19] Funabiki, S., Fujii, T. Fuzzy control of SMES for levelling load power fluctuation based on Lukasiewicz logic Generation, Transmission and Distribution, IEE Proceedings C 1993; 140(2):91 - 95.
[20] Bin Wei, Panpan Chen, Ming Qiu, Hongjie Zhang, Jiahui Zhu, Yanfang Yang, Xiaokang Lai. Experimental investigation into characteristics of micro-SMES' magnet. IEEE Trans. on Applied Superconductivity 2012; 22(3): 5700604.
[21] Alizadeh Pahlavani Mohammad Reza, Mohammadpour Hossine Ali, Shoulaie Abbas. Voltage stabilization of VSI capacitors and voltage sag compensation by SMES using novel switching strategies. Energy 2010; 35(8):3131-3142.
[22] Alizadeh Pahlavani Mohammad Reza, Mohammadpour Hossine Ali. An optimized SVPWM switching strategy for three-level NPC VSI and a novel switching strategy for three-level two-quadrant chopper to stabilize the voltage of capacitors. Energy, 2010; 35(12):4917-4931.